sciendo

Nordic Concrete Federation

© Article authors. This is an open access article distributed under the Creative Commons Attribution-NonCommercial-NoDerivs licens. (http://creaticecommons.org/licenses/by.nc-nd/3.0/).

ISSN online 2545-2819
ISSN print 0800-6377

DOI: 10.2478/ncr-2024-0008

Received: May 3, 2024
Revision received: June 26, 2024
Accepted: June 27, 2024

Comparison and Joint Evaluation of Importance, Redundancy and Robustness Indicators Applied to Aging Prestressed Concrete Bridges

Silvia Sarmiento
M.Sc., Ph.D. Student
Luleå University of Technology (LTU)
Department of Civil, Environmental and Natural Resources Engineering
Luleå University of Technology, 97187 Luleå, Sweden
e-mail: silvia.sarmiento@ltu.se

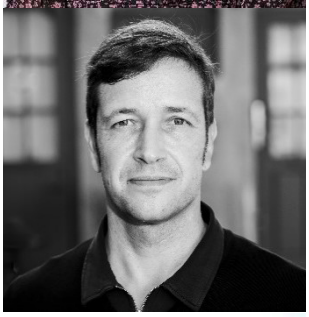

Sebastian Thöns
Ph.D., Professor (LTH)
Division of Structural Engineering
Lund University, SE-221 00, Lund, Sweden
e-mail: sebastian.thons@kstr.lth.se

Jaime González-Libreros
Ph.D., Associate Senior Lecturer (LTU)
Department of Civil, Environmental and Natural Resources Engineering
Luleå University of Technology, 97187 Luleå, Sweden
e-mail: jaime.gozalez@ltu.se

Ivar Björnsson
Ph.D., Senior lecturer (LTH)
Division of Structural Engineering
Lund University, SE-221 00, Lund, Sweden
e-mail: ivar.bjornsson@kstr.lth.se

Gabriel Sas
Ph.D., Professor (LTU)
Department of Civil, Environmental and Natural Resources Engineering
Luleå University of Technology, 97187 Luleå, Sweden
e-mail: Gabriel.sas@ltu.se

ABSTRACT
A bridge failure can result in significant social, economic, and environmental problems; therefore, its reliability and risk management are essential. Bridges' system reliability and risks are governed mainly by their redundancy and robustness, which currently are not adequately included in most design code specifications. Thus, in this study, a comprehensive comparison between relevant importance, redundancy, and robustness indicators found in the literature with different levels of complexity is carried out. The indicators under analysis have been used separately in different studies but have never been addressed together. Therefore, this study presents a joint evaluation of deterministic, reliability- and risk-based indicators to evaluate the differences in interpretation and information provided by the indicators. The approach is exemplified by analyzing a prestressed concrete bridge subjected to continuous degradation due to chloride ingress. A procedure is implemented to couple a metamodel-based reliability approach with a Nonlinear Finite Element Analysis (NLFEA). Based on the analysis performed, the comparison between indicators showed how different interpretations can be obtained depending on the implemented approach. Thus, creating more uniform formulations and agreeing on target values is necessary to help with redundancy and robustness interpretation.

Key words: Importance, redundancy, robustness, prestressed concrete bridge, structural reliability, risk.

1. INTRODUCTION

Bridges are a fundamental component of the transport infrastructure and a key driver of economic growth. Consequently, a bridge failure can lead to severe economic damages and, more critically, the loss of life [1]. A significant number of existing bridges are approaching or have already exceeded their intended lifespans. Over the years, they have been constantly exposed to various degradation agents (such as fatigue loading, aggressive chloride environmental conditions, and overloading) [2]. These agents can significantly reduce their load-carrying capacity [3-7], leaving their safety level uncertain. The uncertainty of bridge safety due to these degradation agents is a clear call for immediate action.

The concepts of importance, redundancy, and robustness have been studied for many years to address the concerns above. The importance of considering these three properties as key structural performance indicators increased after several historical catastrophic failures since they help to minimize the potential for damage propagation and reduce the risk of disproportionate failure events and progressive collapse. Understanding and applying these concepts could be instrumental in preventing such catastrophic failures. In the last decades, studies have been developed in the reliability field applied to assess structure's redundancy and robustness (e.g., [8],

[9]), from which different definitions can be found. These concepts are still controversial [9], [10], and there is no consensus on their adequate levels.

In this study, the term importance refers to the significance of a component or element in maintaining the overall structural integrity (e.g., [11]); redundancy is related to the existence of alternative load paths so that if one element fails, the load is transferred to other elements in the system (e.g., [12]). Moreover, robustness refers to the ability of the system to maintain its structural integrity without excessive changes in system capacity, reliability, or performance in comparison with the damage magnitude (e.g., [13-15]). These concepts can also be related to other factors influencing structural integrity, such as vulnerability, fragility, and resiliency, and their relationship has been studied, for example, by [13], [16] and [17]. As well as the variety in definitions, over the years, several indicators aimed to quantify the redundancy, robustness, and element importance have been developed and further improved.

The variety in available measures are the product of a difference between the indicators concept and their mathematical definition, especially for the case of robustness. The concept of robustness is abstract, allowing for multiple mathematical formulations. These different formulations are intended to address various aspects of robustness treatment, not just the concept itself, such as criteria for robustness, strategies for improving robustness, and methods for assessing or evaluating robustness numerically.

The mathematical definition of these indicators can be obtained from a deterministic, reliability- or risk-based approach. The deterministic approach includes measures defined by responses like displacements [18], resistance [19], [20], and load factors [21], [22], as well as indicators based on structural stiffness, damage development, and energy theory [13] or modified damaged-based measures [23]. Among the drawbacks of existing deterministic-based measures is that they fail to capture the inherent variability and randomness in real-world scenarios, leading to potentially inaccurate structural performance and safety assessments. Consequently, deterministic approaches may overlook critical vulnerabilities and provide an incomplete picture of a structure's redundancy and robustness.

Probabilistic or reliability-based indicators were developed to address the limitations of deterministic-based measures. These measures incorporate the inherent uncertainties in material properties, loading conditions, and environmental factors by using statistical methods to estimate failure probabilities or reliability indexes of intact and damaged systems and individual elements [20], [21], [24]. Conditional probabilities have also been used, e.g., [11], [25], which evaluate the likelihood of failure given specific conditions or events, allowing for a more nuanced understanding of how different factors influence structural integrity.

Furthermore, the risk-based measures integrate failure probabilities with the corresponding consequences, providing a more holistic structural safety evaluation. There are few developed measures or metrics in this category compared to the available deterministic and reliability-based indicators. The most used risk-based measure is the one proposed by [14], and it is acknowledged as one of the most complete [26]. The main drawback of any risk-based indicator is that assessing risks poses challenges due to the diverse ways they can be quantified, encompassing factors like loss of life, monetary cost, or the extent of the damaged area/volume [14], [17], [27].

When evaluating the element importance, redundancy, and robustness of a structure, it is essential to consider the contribution of all structural members; in that way, a path for the load's redistribution can be included. Nonetheless, formulating an explicit performance function is

usually not easy for complex structures, and for such structures, external numerical tools, such as Finite Element (FE) modeling, are necessary. FE modeling has been adopted in many structural reliability problems to simulate the structural behavior and evaluate the performance function [28]. In this case, an implicit function can be used instead, and the interaction of the elements is considered through Finite Element Analysis (FEA) rather than assuming a series-parallel combination of elements [29]. One drawback when using FEM is the high computational cost, a common concern when using Nonlinear Finite Element Analysis (NLFEA), especially when a small probability of failure is expected. In this regard, metamodeling has been an attractive solution to enhance the efficiency of reliability analysis [30], [31]. Examples of these metamodels are Response Surfaces Methods, Support Vector Machine, Neural Networks, and Kriging. The Kriging model has received much attention [31-34] due to its numerical accuracy [35] and because the model provides the corresponding kriging variance.

Based on the abovementioned aspects, this paper presents a first joint evaluation of deterministic, reliability, and risk-based indicators. The main objective is to provide a comprehensive comparison of relevant importance, redundancy, and robustness indicators with different levels of complexity. This comparison is achieved through a case study of a prestressed concrete bridge subjected to capacity degradation due to a chloride attack.

The comparison aims to facilitate a general understanding and overview of the indicators and highlight their differences. The case study serves as an illustrative example, allowing for a detailed examination of how each type of indicator performs under real-world conditions of structural degradation. By applying deterministic, reliability-based, and risk-based measures to the same structure, the case study enables a side-by-side comparison, highlighting the strengths and weaknesses of each approach. The methodology implemented includes the integration of a metamodel-based reliability algorithm that allows and facilitates the integration between the probabilistic assessment and advanced NLFEA.

2. IMPORTANCE, REDUNDANCY, AND ROBUSTNESS INDICATORS

Various metrics associated with the different definitions have been proposed to quantify the indicators. The nature of these indicators' metrics can be classified as deterministic, reliability- or risk-based. This section contains a review of existing indicators on the three main approaches, i.e., deterministic, reliability- and risk-based measures.

2.1 Deterministic measures

Deterministic robustness and redundancy measures from the scientific literature are related to the relation, ratio, or proportion of capacity between the damaged element/system and the intact element/system. For example, in [21] and [22] were proposed three measures (R_{u}, R_{f}, and R_{d}) obtained by the comparison between the system and an individual element's capacity. In this study, those measures based on the load factors (LF) proposed by [21] and [22] are used since they can easily be related to reliability-based measures presented below in Section 3.

The LFs are calculated using Eq. 1 and can be interpreted as the number of times that the design load must be increased for the structure to reach failure. The load factors can be classified as ultimate load factor LF_{u}, functionality load factor LF_{f}, and damage load factor LF_{d}. Each is

compared with the load factor of the most critical element represented by LF_{l}. Following their definition of redundancy and robustness, in [26] it is stated that comparing the load factors would provide objective measures of the system's redundancy and robustness (see Eq. 2).

$$LF_u = P_u / P \qquad LF_d = P_d / P \tag{1}$$

$$R_u = LF_{\mathrm{u}} / LF_l \qquad R_d = LF_d / LF_l \tag{2}$$

where P_{u} and P_{d} are the ultimate load reached by the intact and damaged systems, respectively, and P is the weight load of the design vehicle, R_{u} represents the redundancy ratio and R_{d} represents the robustness ratio given by the damaged condition.

2.2 Reliability-based measures

In previous studies, probabilistic concepts have been introduced into the quantifications of importance, redundancy, and robustness to include part of the existing uncertainties [20-22], [24], [36]. In [21] re-formulated the expressions in Eq. 2 using the reliability index β, which can be defined as the system and component reliability differences, denoted as $\Delta\beta_{\mathrm{u}}$ and $\Delta\beta_{F_{\mathrm{S}}|F_{\mathrm{l}}}$ for the intact and damaged states of the system, respectively. These reliability differences can be obtained using the following expression:

$$\Delta\beta_{\mathrm{u}} = \beta_{\mathrm{S}} - \beta_{\mathrm{l}} \quad \Delta\beta_{\mathrm{d}} = \beta_{F_{\mathrm{S}}|F_{\mathrm{l}}} - \beta_{\mathrm{l}} \tag{3}$$

where β_{S} and β_{d} are the reliability indices of the intact (S), and damaged ($F_{\mathrm{S}}|F_{\mathrm{l}}$) systems, respectively, and β_{l} is the reliability index of the element. Eq. 3 can be expressed as a function of the time t as:

$$\Delta\beta_{\mathrm{u}}(t) = \beta_{\mathrm{S}}(t) - \beta_{\mathrm{l}}(t) \quad \Delta\beta_{\mathrm{d}}(t) = \beta_{F_{\mathrm{S}}|F_{\mathrm{l}}}(t) - \beta_{\mathrm{l}}(t) \tag{4}$$

Additionally, in [37] is proposed two system performance indicators, IR_{S} and IR_{d}, and their values are obtained using Eq. 5. The measures were proposed as indicators of the redundancy and robustness of structural systems; however, they can be better interpreted as importance measures. Higher values of IR_{S} and IR_{d} are obtained when considered the failure of an element with higher importance compared to less important elements.

$$IR_{\mathrm{S}} = P(F_{\mathrm{S}})/P(F_{\mathrm{l}}) \qquad IR_{\mathrm{d}} = P(F_{\mathrm{S}}|F_{\mathrm{l}})/P(F_{\mathrm{S}}) \tag{5}$$

where $P(F_{\mathrm{S}})$ is the probability of the intact system failure F_{S}, $P(F_{\mathrm{S}}|F_{\mathrm{l}})$ is the probability of the system failure given the element failure F_{l}, and $P(F_{\mathrm{l}})$ is the probability of the element failure.

Similarly, an importance measure was proposed by [20]. Originally, the indicator was denominated as a redundancy index (RI) and its definition is close to IR_{d} (see Eq. 6). The difference is that RI is expressed as a difference ratio, and IR_{d} is a ratio only. However, both provide a degree of importance of an element in the system's reliability. Additionally, the authors obtained a redundancy reliability index β_{R}, which is an inverted version of RI and expressed in terms of reliability indexes, see also Eq. 6.

$$RI = (P(F_{\mathrm{S}}|F_{\mathrm{l}}) - P(F_{\mathrm{S}}))/P(F_{\mathrm{S}}) \qquad \beta_{\mathrm{r}} = \beta_{\mathrm{S}}/\left(\beta_{\mathrm{S}} - \beta_{F_{\mathrm{S}}|F_{\mathrm{l}}}\right) \tag{6}$$

As a different approach, conditional probabilities have also been implemented to obtain system performance indicators. For instance, [11], [37], and [38] defined redundancy as the probability of the system failure with the failed element removed. Furthermore, [11] presented a measure named the single element importance ($\mathrm{SEI_i}$), which is defined by Eq. 7. $\mathrm{SEI_i}$ provides the

difference between the failure probabilities of the intact system and the system considering the failure of a member i.

$$\mathrm{SEI_i} = \Pr[C(t)|\Psi(t) = (\bar{F}_1 \cap \ldots \cap \bar{F}_{i-1} \cap \bar{F}_i \cap \bar{F}_{i+1} \cap \ldots \cap \bar{F}_n)] - \Pr[C(t)|\Psi(t) = \psi_1] \quad (7)$$

where, $\Pr[C(t)|\Psi(t)]$ is the probability of collapse $C(t)$ at specific time t given a deterioration case $\Psi(t), \Psi(t) = (\bar{F}_1 \cap \ldots \cap \bar{F}_{i-1} \cap \bar{F}_i \cap \bar{F}_{i+1} \cap \ldots \cap \bar{F}_n)$ represents the deterioration case in which the element i has failed, and $\Psi(t) = \psi_1$ is the case in which all the elements are intact. Eq. 7 may be adjusted to the previous introduced denotation and expressed as:

$$\mathrm{SEI_i} = P(F_S|F_i)(t) - P(F_S)(t) \quad (8)$$

2.3 Risk-based measures

Risk-based approaches for determining robustness are based on considering both the probability of element and system collapse, including the economic and societal consequences. The risk quantification can be summarized by Eq. 9:

$$R = \sum_{i=1}^{n}\sum_{j=1}^{m}\sum_{k=1}^{h} P\left(F_k\middle|D_j\right) \cdot P\left(D_j\middle|H_i\right) \cdot P(H_i) \cdot C(F_k, D_j) \quad (9)$$

where, R is the total risk, D, H and F represent sets of m damages, n hazards, and h failure events, respectively, and $C(F_k, D_j)$ is the cost of failure and damage, in which the consequences of damage and collapse may be given monetary values.

In [14] the authors proposed a robustness index taking basis in risk analysis and with the distinction of direct and indirect, i.e., follow-up, consequences expressed by Eq. 10. The robustness index ranges from 0.0 to 1.0, for which a value of 1.0 indicates very high robustness corresponding to negligible indirect, i.e., follow-up consequences. The direct and indirect risks can be calculated for different points using Eqs. 11-12. Finally, the total risk caused by the failure of the element is given by Eq. 13.

$$I_{rob} = R_{Dir}/(R_{Dir} + R_{Ind}) \quad (10)$$

$$R_{Dir}(t) = \sum_{i=1}^{n}\sum_{j=1}^{m} P\left(D_j(t)\middle|H_i(t)\right) \cdot P(H_i(t)) \cdot C_{Dir}(t) \quad (11)$$

$$R_{Ind}(t) = \sum_{i=1}^{n}\sum_{j=1}^{m}\sum_{k=1}^{h} P\left(F_k\middle|D_j(t)\right) \cdot P\left(D_j(t)\middle|H_i(t)\right) \cdot P(H_i(t)) \cdot C_{Ind}(t) \quad (12)$$

$$R(t) = R_{Dir}(t) + R_{Ind}(t) \quad (13)$$

where R_{Dir} is the direct risk related to element failure, and R_{Ind} is the indirect risk related to the collapse of the system, $C_{Dir}(t)$ are the direct consequences associated with the failure of the element (i.e., the cost to replace the element); and $C_{Ind}(t)$ are the indirect consequences at time t caused by the failure of the system (i.e., the cost to rebuild the subsequent system, safety loss and environment loss).

3. STRUCTURAL RELIABILITY AND RISK ANALYSES

The methodology implemented in this study can be divided into three primary analyses: structural, reliability, and risk analyses, and a detailed description of them is presented in Sections 3.1-3.3. Each analysis is explained by targeting the case of prestressed concrete structures subjected to material degradation due to chloride attack.

3.1 Structural analysis

Modeling of failure scenarios
The modeling of failure scenarios is performed considering the different exposures and loads to which the structure is subjected. Furthermore, the critical element(s) are identified, i.e., the elements most probable to fail first due to the identified exposure(s). Given an exposure, the critical elements are identified considering: (1). the element(s) with higher stresses, given the normal loads, and (2). the element(s) with higher time and magnitude of exposure. Once the critical elements are identified, the damaged scenario of the structure can be analyzed by considering that the critical elements have failed.

Two system states and one element state are analyzed to determine the system performance indicators. The first system state corresponds to the intact structure, representing the structure under analysis subjected to normal loading before exposure to any hazard. The element state corresponds to the study of the critical element(s) due to a determined exposure, and the second system state corresponds to the damaged structure, which represents the case in which the critical elements have failed and are discarded as a part of the structure.

Structural system model through FEM
In this study, the structural system is modeled through a Finite Element (FE) software, and a Nonlinear FE Analysis (NLFEA) is carried out to study the system's failure. From the NLFEA, the overall resistance of the structural system is obtained, as well as the identification of the critical sections and elements. For this study, the software ATENA Studio v.5.9 [39] was used, which is specialized in NLFEA applied to concrete structures. Previous publications have demonstrated that ATENA can realistically simulate the concrete behavior in both ductile and brittle failure modes [40], [41], and the constitutive models in ATENA have been implemented in the numerical analyses of a wide range of concrete structures, including full-scale bridges (e.g., [42-44]), and reliability analysis [45] with satisfactory results.

The deterioration of the system capacity due to the reinforcement corrosion is also included in the FE model, as well as the prestressing losses. The prestressing losses are calculated following the AASHTO LRFD [46] and discounted to the initial prestressing force. Furthermore, the force after losses is applied to the tendons in the FE model. The reinforcement corrosion is evaluated from the parameters of the surrounding environment, specified as a special boundary condition. The diffusion in the structure is governed by additional factors such as concrete cover thickness, water-to-binder ratio, and crack propagation. The time of corrosion initiation is calculated according to [47] and, e.g., [48] as:

$$C(x,t) = C_{\mathrm{S}}\left[1 - \mathrm{erf}\left(\frac{x}{2\sqrt{D_{\mathrm{m}}(t)f(w)t}}\right)\right] \tag{14}$$

where C_{S} is the chloride content at the surface in kg/m^3, $D_{\mathrm{m}}(t)$ is the average diffusion coefficient at time t in m^2/s, x is the distance from the surface in m, and $f(w)$ is a function that introduces corrosion acceleration due to cracking. The propagation phase is controlled by the corrosion rate. The chloride ingress depends on the corrosion current density i_{corr} (in μA/cm^2) and chloride concentration at the reinforcement level in the concrete. A more detailed explanation of the chloride-induced corrosion implemented in ATENA can be found in [49].

3.2 Reliability analysis

After obtaining the failure scenarios, the reliability analysis is performed, which aims to quantify the safety level of a determined structure. This safety level is expressed in terms of the reliability index (β) and its associated probability of failure ($P(F)$). The failure event F of the element or system can be formulated in terms of the random variables resistance R and load S as:

$$F: g(\boldsymbol{X}) = R - S \leq 0 \tag{15}$$

$g(\boldsymbol{X})$ is the limit state function, and $\boldsymbol{X}$ is the vector of random variables.

In this study, a metamodel-based reliability analysis is performed to obtain the values of $P(F)$ and β, which is described in Section 3.2.1. When more than one critical element is identified, the individual elements' failure is formulated separately, and the failure of the elements and system should be represented by structural system reliability modeling. The system probability can be calculated with the individual element limit state functions $g_{F,\mathrm{i_c},\mathrm{j_c}}$ for $n_{\mathrm{j_c}}$ parallel and $n_{\mathrm{i_c}}$ series elements:

$$P(F_{\mathrm{S}}) = P\left(\bigcap_{\mathrm{j_c}}^{\mathrm{n_{j_c}}} \bigcup_{\mathrm{i_c}}^{\mathrm{n_{i_c}}} \left\{g_{F,\mathrm{i_c},\mathrm{j_c}} \leq 0\right\}\right) \tag{16}$$

Metamodel-based Reliability Analysis

A metamodel-based reliability methodology consists mainly of substituting the original limit state for a surrogate model. This substitution allows the assessment of the limit-state function without having to perform additional FEM evaluations, thus, obtaining a reasonable computational cost. The three critical steps of a metamodel-based reliability algorithm are (1). Implementation of an experiment design (*DoE*) to get the Experimental Points (*EP*s), (2). Use a regression method to obtain a surrogate model (metamodel), and 3. Calculation of β and $P(F)$ values.

The kriging metamodel was chosen due to its exact interpolation nature and it has demonstrated good efficiency in structural systems reliability problems [31], [50]. This model is also known as the Gaussian Process Regression, and it has received particular attention in the structural reliability methods based on metamodels. In reliability, kriging regression aims to approximate the performance function $g(\boldsymbol{X})$, based on a given dataset, into a model $\hat{g}(\boldsymbol{X})$ that combines a regression model and a stochastic process, as shown in Eq. 17.

$$\hat{g}(x_{\mathrm{i}}) = f^T(x_{\mathrm{i}})\hat{\beta} + z(x_{\mathrm{i}}) \tag{17}$$

where, $f^T(x_{\mathrm{i}})$ is the basis function, $\hat{\beta}$ is the vector of the regression coefficients, and $z(x_{\mathrm{i}})$ is a stationary Gaussian process with zero mean, variance ${\sigma_{\mathrm{Z}}}^2$, and covariance expressed by Eq. 18:

$$CoV\left[z(x_{\mathrm{i}}), z(x_{\mathrm{j}})\right] = \sigma_{\mathrm{Z}}^2 \boldsymbol{R}(x_{\mathrm{i}}, x_{\mathrm{j}}; \boldsymbol{\theta}) \tag{18}$$

where, $\mathbf{R}(x_{\mathrm{i}}, x_{\mathrm{j}}; \boldsymbol{\theta})$ is a correlation function between the experimental points x_{i} and x_{j}, and $\boldsymbol{\theta}$ is a vector of undetermined correlation parameters.

The trend of the basis function $f^T(x_{\mathrm{i}})$ is usually adopted as constant ($\hat{\beta}_{\mathrm{o}}$); in that case, the model is called ordinary kriging. Other trends, such as the linear or quadratic polynomial, can also be used. In this paper, the ordinary kriging was adopted. The experimental points to which the model fits were generated using the Latin Hypercube Design (LHD) due to its space-filling properties and flexibility in choosing the number of experimental points. LHD is used for the first iteration, generating $2n + 1$ points, being n the number of random variables. For the subsequent iterations, the learning function $U(\boldsymbol{X})$ shown in Eq. 19 was used:

$$U(\boldsymbol{X}) = |\hat{g}(x)|/\sigma_{\hat{g}}(x) \tag{19}$$

where, $\hat{g}(\boldsymbol{X})$ is the kriging-limit state function, and $\sigma_{\hat{g}}(\boldsymbol{X})$ is the kriging standard deviation.

The learning function's objective is to identify the best next point to be added to the EPs. This can be done by finding the point that minimizes the function $U(\boldsymbol{X})$, as shown in Eq. 20 since a small value of $U(\boldsymbol{X})$ means either $\hat{g}(\boldsymbol{X})$ is close to zero or $\sigma_{\hat{g}}(\boldsymbol{X})$ is significant. A value that minimizes the learning function will have a higher probability of being close to the limit $\hat{g}(\boldsymbol{X}) = 0$ (the region of interest) [30]. Once the best point x_{next} is identified, it is added to the EPs, improving the accuracy of the metamodel. This procedure iterates until the stopping criterion $U_{\min}(\boldsymbol{X}) \geq 2$ is satisfied. The last criterion is used since $U(\boldsymbol{X}) = 2$ corresponds to the case of the sample being correctly classified with a probability of $\Phi(2) = 0.977$.

$$x_{\text{next}} = \arg\min_{\text{x}} U(\boldsymbol{X}) \tag{20}$$

The prediction error, i.e., the metamodel uncertainty, is modeled and accounted for in the reliability analysis by randomly generating the prediction value from the prediction distribution, which is assumed to be normal with mean $\mu_{\hat{g}(\boldsymbol{X})}$ and variance $\sigma^2_{\hat{g}(x)}$:

$$\mu_{\hat{g}(x)} = f^{\mathrm{T}}(\boldsymbol{X})\hat{\beta} + r(\boldsymbol{X})^{\mathrm{T}}\boldsymbol{R}^{-1}(g - F\hat{\beta}) \tag{21}$$

$$\sigma^2_{\hat{g}(\boldsymbol{X})} = \sigma_Z^2\{1 - r(\boldsymbol{X})^{\mathrm{T}}\boldsymbol{R}^{-1}r(\boldsymbol{X}) + [F^{\mathrm{T}}\boldsymbol{R}^{-1}r(\boldsymbol{X}) - f(\boldsymbol{X})]^{\mathrm{T}}(F^{\mathrm{T}}\boldsymbol{R}^{-1}r(\boldsymbol{X})F)^{-1}[F^{\mathrm{T}}\boldsymbol{R}^{-1}r(\boldsymbol{X}) - f(\boldsymbol{X})]\} \tag{22}$$

where, g is the vector of the original limit-state function responses, $r(x)$ is the vector of cross-correlations between the prediction point $\boldsymbol{X}$ and each one of the observations and F is the design matrix of the Kriging metamodel trend.

The coefficient of determination R^2 is calculated to check the data fitting of the metamodel, where values of R^2 closer to 1 represent a better fitting of the data. A good metamodel is not just the one that succeeds in fitting the data but can predict the response in points where there is no information. Thus, techniques such as Cross-Validation (CV) (commonly used in Machine Learning) have been developed to validate and improve the metamodel's construction. In this study, a ten times 10-fold CV was implemented, and an effective measure of error was used, that is the squared predictability correlation coefficient Q^2. For each fold, the coefficient Q^2 is obtained, then the average of all the coefficients is calculated. Generally, a good fitting and prediction of the data are given by coefficients $R^2$and Q^2 with values above or equal to 0.7. If values below 0.7 are obtained for either R^2 or Q^2, additional *EPs* need to be included in the metamodel to increase its accuracy.

Once the metamodel is constructed and its accuracy is verified, a Monte Carlo simulation is implemented to evaluate the probability of failure, using Eq. 23:

$$P(F) = N_{\hat{g}\leq 0}/N_{\text{sim}} \tag{23}$$

where, $N_{\hat{g}\leq 0}$ is the number of times the limit-state function had values less or equal to zero, i.e., was in the failure zone, and N_{sim} is the total number of simulations.

3.3 Risk analysis

The risk analysis builds upon the structural reliability analysis, includes the consequence modeling for the failure scenarios, and associates the consequences with the damage and failure states of elements and the system. Determining the risks associated with specific bridge damage or failure scenarios requires identifying and quantifying the consequences of the corresponding end states.

In general, consequences related to risk-based robustness measures are divided into direct and indirect consequences [14], denominated before as C_{dir} and C_{ind}, respectively. The exact definition of both depends on how the system and scenario are modeled; however, the former is commonly associated with localized failure, while the latter considers any subsequent propagation of the damage in the structure, e.g., bridge failure. Different approaches are possible to model and quantify these consequences; however, it is common to consider distinct consequence types, including (1) human, (2) economic, and (3) environmental impacts [51]. An overview of relevant consequences can be seen in [52].

Directly combining bridge damage and failure consequences requires transforming to standard units, e.g., monetary value. In Sweden, the Transport Administration (*Trafikverket*) provides socio-economic cost-benefit models for various impacts on the transportation infrastructure, which are updated regularly; these include traffic delays and disruptions, environmental impacts, and traffic safety and accident costs [53]. Models for determining human casualties (and costs), traffic management costs, and repair/rebuild costs for bridges can be found in the literature [52], [54] and [55].

The consequences related to an exposure event includes the repair costs (C_{rep}) of the element and system (re-building costs), the traffic delay costs (C_{TD}) for vehicles unable to pass over and/or under a failed bridge, and the potential human injuries or causalities (C_{HC}) associated with bridge failure. The repair costs, C_{rep}, will depend on the extent of damage and should be determined depending on the type of repair needed and the respective costs. For simplification, this cost may be expressed as a fraction of the rebuild cost, C_{new} (see Eq. 24), or it can also be estimated based on the original cost or a reference value presented as a ratio of the bridge deck area.

$$C_{\mathrm{rep}} = \delta \cdot C_{\mathrm{new}} \tag{24}$$

where $\delta << 1$ can, as a further simplification, be estimated based on the extent of damage in relation to the bridge size.

The severity of consequences associated with traffic disruptions requires estimating the additional (or delay) time experienced by traffic users because of detours or congestion following the bridge's collapse. The following monetary costs can be distinguished [52]:

$$C_{\mathrm{TD}} = (\sum VT \cdot n) \cdot t_{\mathrm{d}} \tag{25}$$

with,

$$t_{\mathrm{d}} = L_{\mathrm{d}} \cdot v \tag{26}$$

where VT is the value of time for vehicle time (cost unit/time), n is the corresponding traffic intensity (number of vehicles), t_d is the expected additional travel time (or delay), L_{d} is the detour length, and v is the average traffic speed.

For the human causalities, three scenarios are considered: (1) deaths/injuries to persons on the bridge at the time of the collapse, (2) deaths/injuries to persons underneath the bridge at collapse, and (3) death/injuries related to vehicles colliding with the collapsed bridge. The estimated number of casualties N for all cases can be determined from the following equation:

$$N = P \cdot ((n \cdot L)/v) \cdot O \tag{27}$$

where, P is the probability of a specific casualty type, L is the reference length (distance), v is the average traffic speed, and O is the average vehicle occupancy (persons/vehicle). The relevant input for each scenario is provided in [52].
It should be identified among the different consequences considered (C_{rep}, C_{TD}, and C_{HC}), which are direct and indirect consequences, and obtain the C_{Dir} and C_{Ind} total values. When dealing with time-dependent risks of an event that occurs in the future, it should be discounted to the present monetary value (C_{PV}) of the consequence and determine $C_{\mathrm{Dir}}(t)$ and $C_{\mathrm{Ind}}(t)$ using the following relation:

$$C_{\mathrm{Dir}}(t) = C_{\mathrm{PV,Dir}} \cdot (1+r)^{\mathrm{t}} \text{ and } C_{\mathrm{Ind}}(t) = C_{\mathrm{PV,Ind}} \cdot (1+r)^{\mathrm{t}} \tag{28}$$

where t is the year under analysis and r is the annual discount rate, which can vary depending on economic, social, and political factors [56].

Once the consequence modeling is performed and the $C_{\mathrm{Dir}}(t)$ and $C_{\mathrm{Ind}}(t)$ values are known, the respective indirect and direct risks can be assessed. Risk values are obtained using Eqs. 11-13, which combine the probabilities of failure obtained through the methodology described in Section 3.2.2 and the associated consequences. As a final step in the risk analysis, the robustness index of the structure I_{rob} presented in Eq. 10, Section 2, is calculated.

4. EXAMPLE APPLICATION

An example of a prestressed concrete bridge is used in this study to evaluate the differences between the indicators presented in Section 2. The structure under analysis is subjected to a constant chloride exposure, and therefore a resistance degradation is considered. The indicators are evaluated for different points in time (5, 25, and 50 years) to study how the values change for different levels of corrosion.

4.1 General description

The structure under study is located in Colombia, and it was chosen as a case study due to the availability of design information. The bridge belongs to a third-class road in the country, which means the traffic volume is low; however, heavy trucks can still transit over the bridge. The structure was designed in 1976 following the AASHTO (1965) [57] specifications.

The superstructure consists of four parallel pre-fabricated prestressed concrete beams and a reinforced concrete deck. The bridge has one span of 26 m, whose cross-section is shown in. The detailed cross-section of each beam and the reinforcement configuration are presented in Figure 1, as well as the reinforcement configuration. The beams were designed with a compressive strength f_{c}= 28 MPa, and an elasticity modulus E_{c} = 30.3 MPa. The deck's concrete has a compressive strength of f_{c} = 21 MPa and modulus of elasticity of E_{c} = 27.5 MPa. Yield strength of f_{y} = 370 MPa was specified for the reinforcement bars.

The prestressed cables comprised seven 9.5 mm diameter strands with ultimate tensile strength and modulus of elasticity f_{pu}= 1890 MPa and E_p= 197 GPa, respectively. Seven cables were specified for each beam with an initial prestressing force of 420 kN. The cable profile and the shear reinforcement distribution are shown in Figure 1c. The structure is submitted to traffic loads, which were defined based on the design loads, corresponding to the vehicle HL-93, and a lane load is considered and uniformly distributed on the bridge deck, and its magnitude is specified as q=9 kN/m. The vehicle HL-93 is constituted by three axle loads with a 4.3 m spacing.

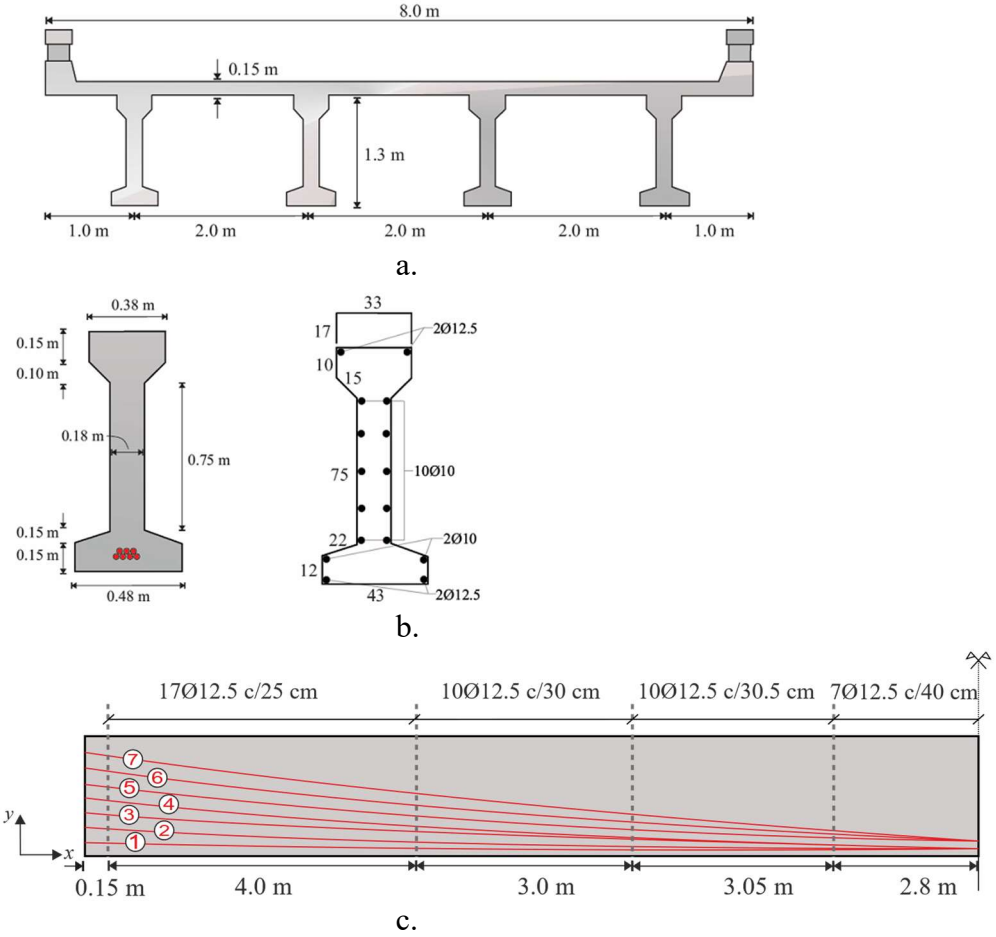

Figure 1 – Bridge geometry and detailing a. cross-section view, b. prestressed beam at mid-span and reinforcement bars and stirrups configuration and c. cables profile and shear reinforcement distribution.

4.2 Modeling of failure scenarios

The failure scenarios are modeled considering that the structure is under two main exposures: traffic loads and chloride ingress. It is well known that cracking of the concrete highly influences the chloride attack, and for prestressed structures micro-cracking can be a product of differential shrinkage and creep [58]. Therefore, the elements more likely to fail were determined considering the following aspects:

1) The bridge failure herein studied corresponds to a flexural failure produced once the reinforcement and tendons reach the maximum strain.

2) Corrosion is propagated equally for the four beams; however, the traffic load is located in the critical flexure point, which makes the tendons on that section more probable to fail.
3) For bending at the critical section, the bottom bars and tendons handle more stress than the others; however, the tendons are the elements with the highest level of stress in comparison with the reinforcement bars.
4) At the critical section, four of the seven tendons are located closer to the external surface, where the chlorides ingress; hence, they have an earlier chloride ingress and, therefore, more exposure time.

Following the failure scenario described, the damaged state of the structure is represented by the bridge system without the four failed tendons in the external beam (see Figure 2).

Scenario representation	Physical characteristics	Consequences
Element damage and failure states 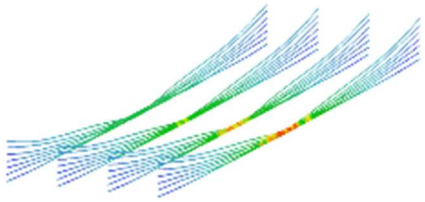 Corrosion level in tendons	Failure of tendon and reinforcement (see Section 4.4., Eqs. 30 and 33).	**Direct consequences:** Cost to rebuild the system (see Section 3.3., Eq. 24)
System damage and failure states 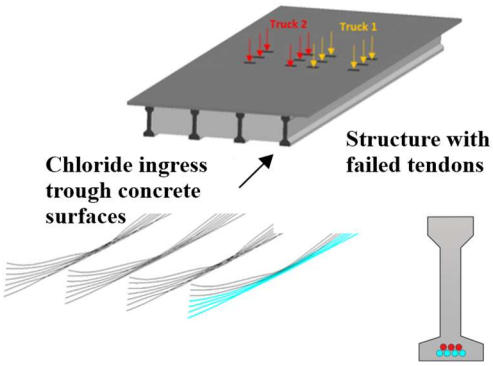 Failed tendons highlighted in cyan color	Failure of the intact system (see Section 4.4., Eq. 31) Failure of the damaged system (see Section 4.4., and Eq. 32)	**Indirect consequences:** Cost of traffic disruption (see Section 3.3., Eqs. 25 and 26) and Human causalities (see Section 3.3., and Eq. 27)

Figure 2 – Scenario representation with element and system damage and failure states and allocated consequences.

4.3 Structural analysis

Two FE models were developed to represent the two systems' states, i.e., intact and damaged systems. The intact state considers the bridge superstructure with all the structural elements. Furthermore, the damaged state of the system considers the failure of the four tendons mentioned in the previous section; therefore, the failed tendons are removed from the FE model. Also, for the system's damaged state, the degradation model over time due to chloride ingress is included.

The model mesh consisted of continuum 3D solids elements (the isoparametric 8-node brick with eight integration points) with an average size of 15x15x15 cm^3 and linear interpolation, shown in Figure 3. The tendons and bar reinforcement were modeled as embedded truss elements.

Furthermore, steel plates representing the bearings at the support were included in the model. The prestressing of the cables was modeled as an initial strain ε_{ini}, which value is calculated through the expression Eq. 29:

$$\varepsilon_{\mathrm{ini}} = \sigma_{\mathrm{p}}/E_{\mathrm{ps}} \quad \text{and} \quad \sigma_{\mathrm{p}} = P_{\mathrm{e}}/A_{\mathrm{ps,i}} \tag{29}$$

where, P_{e} is the prestressing force after losses, and $A_{\mathrm{ps,i}}$ is the area of the prestressing tendon i.

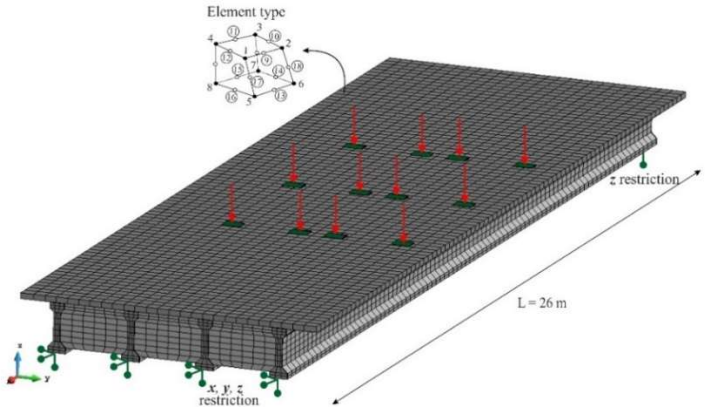

Figure 3. System FEM.

4.4 Reliability analysis

The random variables for the case study are listed in Table 1, as well as the probabilistic distribution and the respective parameters, which were based on previous studies [59-64] and the JCSS [65] guideline.

Table 1 – Random variables.

Variable	Dist.	μ_x	v_x	Variable	Dist.	μ_x	v_x
f_{c} (MPa)	Log-normal	38.2	0.18	W_{g} (kN/m^2)	Normal	15.8	0.1
f_{t} (MPa)	Weibull	2.8	0.18	D_{m}(m^2/2)	Normal	1.2×10^{-12}	0.2
E_{c} (MPa)	Log-normal	33598.7	0.15	C_{S}(%)	Normal	2.5×10^{-2}	0.18
G_{f} (N/m)	Weibull	140.6	0.2	C_{cr}(%)	Normal	4×10^{-3}	0.22
A_{ps} (m^2)	Normal	4.9×10^{-4}	0.013	M_{R}	Log- normal	1.04	0.15
P_{ve} (kN)	Gumbel	67	0.25	M_{L}	Log-normal	1.0	0.2
P_{e}(kN)	Normal	429.3	0.05				

The parameters assumed to be random variables are properties of the concrete (f_{c}, f_{t}, E_{c}, G_{f}), the area of the prestressing tendons (A_{ps}), loads such as self-weight (W_{g}), prestressing force (P_{e}), vehicle weight P_{ve} and corrosion parameters (D_{m}, C_{S}, and C_{cr}). For the corrosion parameters, it was assumed that the level of aggressiveness of the chloride is low, i.e., for structures placed at 2.84 km or more from the sea. The probabilistic values were taken from [66], [67]. The correlation between the concrete properties was considered, with coefficients chosen based on [64].

Different limit state functions are formulated based on Eq. 15, for the tendon ($g_{F_T}(\boldsymbol{X}, \boldsymbol{t})$), the intact system ($g_{F_S}(\boldsymbol{X})$), and the damaged system ($g_{F_{\mathrm{S}}|F_{\mathrm{T}}}(\boldsymbol{X}, t)$) as:

$$F_{\mathrm{T}}: g_{F_{\mathrm{T}}}(\boldsymbol{X}, t) = M_{\mathrm{R}} R_{\mathrm{T}}(t) - M_{\mathrm{L}} L \leq 0 \tag{30}$$

$$F_{\mathrm{S}}: \; g_{F_S}(\boldsymbol{X}) = M_{\mathrm{R}} R_{\mathrm{S}} - M_{\mathrm{L}} L \tag{31}$$

$$F_{\mathrm{S}}|F_{\mathrm{T}}: \; g_{F_{\mathrm{S}}|F_{\mathrm{T}}}(\boldsymbol{X}, t) = M_{\mathrm{R}} R_{\mathrm{S}}(F_{\mathrm{T}}, t) - M_{\mathrm{L}} L \tag{32}$$

where, R_{S} and $R_{\mathrm{S}}(F_{\mathrm{T}}, t)$ are the intact and damage systems resistance at the time t, respectively, M_{R} is the FEM model uncertainty, and M_{L} is the uncertainty of the loading model L.

The failed tendons are located at the bottom of the beam in the critical section. Due to the full correlation of the loading, the resistance, and the high correlation of the section loss induced by the chloride exposure and corrosion, the system failure of the four tendons equals the individual probabilities of failure, i.e.:

$$D_{\mathrm{T,S}} = (F_{\mathrm{T},1} \cap F_{\mathrm{T},2} \cap F_{\mathrm{T},3} \cap F_{\mathrm{T},4}) = \min_{\mathrm{i}=1:4}\{P(F_{\mathrm{T,i}})\} = P(F_{\mathrm{T,i}}) \tag{33}$$

with $\rho\left(F_{\mathrm{T,i_T}}, F_{\mathrm{T,i_T+1}}\right) = 1.0$.

Results from the reliability analysis

The reliability index β, the probability of failure $P(F)$, and the number of limit state function evaluations (n_{calls}), obtained from the reliability analysis are presented in Table 2. The factors R^2 and Q^2, for all cases and the different points in time, obtained factors with values 1.0, which means that the model could accurately fit and predict the data.

Table 2 – Results from reliability analysis for the element (tendon), intact and damaged system.

	Intact system	Tendons			Damaged system		
		5 years	25 years	50 years	5 years	25 years	50 years
$\beta(t)$	6.46	5.03	4.02	2.97	2.1	1.95	1.78
$P(F)(t)$	1.3×10^{-11}	2.5×10^{-7}	2.9×10^{-5}	1.5×10^{-3}	1.8×10^{-2}	2.5×10^{-2}	3.7×10^{-2}
n_{calls}	60	37	55	73	218	136	98

The reliability results showed how the reliability of the damaged system is significantly lower than corresponding values of the tendons and intact systems. Thus, the results show that the failure of the tendons and the continuous degradation of the system's capacity due to the corrosion of remaining elements significantly impact the reliability of the structure.

4.5 Risk analysis

Direct consequences

For this case study, the direct consequences were treated as the cost of repairing the external prestressed beam, which has suffered the loss of the tendons and rebars. The cost of the prestressed beam repair ($C_{\mathrm{Dir},1}$) was based on previous studies which have pointed out that, on average, a prestressed beam replacement costs 8000 USD per ft of the beam (≈ 26247 USD per m), and it takes approximately one to two months to complete [68]. This value was multiplied by the span of the bridge to obtain the total beam replacement cost. The cost of delay due to the beam's

replacement ($C_{\mathrm{Dir},2}$) was considered a direct consequence since a significant portion of the bridge becomes unusable while it is being repaired.

Indirect consequences
The indirect consequences include the costs related to the extension of damages in the structure. Therefore, in this study, the following costs were considered:

- The rebuilt cost ($C_{\mathrm{Ind},1}$) of the system. This cost can be obtained by considering the current cost of building a new superstructure or the value of replacing a prestressed concrete beam multiplied by the total number of beams plus a percentage related to the deck and transversal elements replacement. For the case study, the cost of replacing the whole superstructure was obtained by multiplying the cost of the beam's replacement by four (4) (since there are four beams) plus a 20% percentage representing the slab replacement.
- Cost of traffic disruption ($C_{\mathrm{Ind},2}$), which was considered and obtained using Eq. 25. However, the delayed traffic passing under the bridge was discarded since the bridge crosses a river, and there is no traffic below the structure. The costs were calculated considering the closest roads leading to Barrancabermeja, where a total detour length of 56 km was determined (corresponding to ≈ 2 hours of additional travel time).
- The number of human causalities was obtained using Eq. 27, considering an average vehicle velocity of 40 km/h and a traffic volume of 100 vehicles/day. The cost per fatality and severe injury in Colombia in 2016 was estimated at 17,5 million USD for 142 reported fatalities and serious injuries [69]. Considering this value, one fatality or injury is assumed to cost about 1.24×10^5 USD.

The costs for the different points in time were obtained using a discount rate of 3%. Table 3 and Table 4 summarize the consequences at the different points in time related to the structure, and human causalities, respectively.

Table 3 – Consequences related to the structure.(USD)

	Present value	5 years	25 years	50 years
Replacement cost beam ($C_{\mathrm{Dir},1}$)	6.8×10^5	5.9×10^5	3.3×10^5	1.6×10^5
Delay cost 1 ($C_{\mathrm{Dir},2}$)	2.4×10^5	2.1×10^5	1.2×10^5	5.5×10^4
Replacement cost of superstructure ($C_{\mathrm{Ind},1}$)	2.9×10^6	2.5×10^6	1.4×10^6	6.5×10^5
Delay cost 2 ($C_{\mathrm{Ind},2}$)	1.0×10^6	8.7×10^5	4.8×10^5	2.3×10^5

Table 4 – Consequences related to the human causalities. (USD)

			Present value	5 years	25 years	50 years
Human Causalities	N_{f} = 83	C_{f} =	10.3×10^6	8.9×10^6	4.9×10^6	2.4×10^6
	N_{s} = 28	C_{s} =	3.5×10^6	3.0×10^6	1.7×10^6	8.0×10^5
	Total ($C_{\mathrm{Ind},3}$) =		13.8×10^6	1.2×10^7	6.6×10^6	3.2×10^6

Determination of risk
To calculate the direct R_{Dir} and indirect R_{Ind} risks, it can be used the expressions below:

$$R_{\mathrm{Dir}} = (C_{\mathrm{Dir},1} + C_{\mathrm{Dir},2}) \cdot P(F_{\mathrm{T}}) \tag{34}$$

$$R_{\mathrm{Ind}} = (C_{\mathrm{Ind},1} + C_{\mathrm{Ind},2} + C_{\mathrm{Ind},3}) \cdot P(F_{\mathrm{S}}) \tag{35}$$

with,

$$P(F_S) = P(F_S|F_T) \cdot P(F_T) \quad (36)$$

where $P(F_T)$ is the tendons' probability of failure, $P(F_S|F_T)$ is the conditional probability of the bridge system failure due to the tendons' failure, and $P(F_S)$ is the probability of failure of the system.

4.6 Importance, redundancy and robustness indicators

Deterministic indicators

With the deterministic approach, presented in Section 2, the redundancy and robustness indicators R_u and R_d are calculated based on the load factors LF_l, LF_u, LF_d related to the tendons, intact and damaged bridge systems, respectively. Both the redundancy and robustness indicators show an increase in time (see Figure 4b.) due to the more rapid drop of the LF_l values through the years (in comparison with LF_u and LF_d). The LF_l behavior is obtained due to the direct influence of the chloride ingress on the components' system, which results in more significant losses on its bending capacity compared to the bridge system.

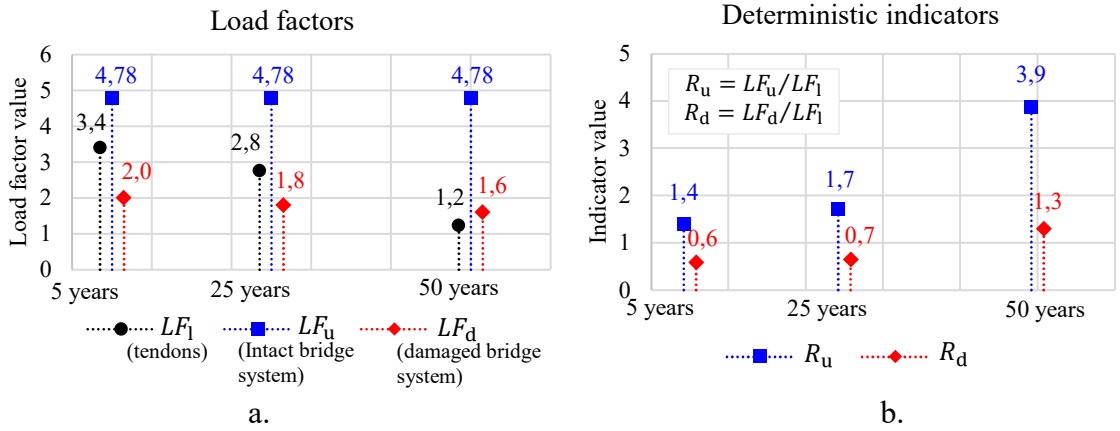

Figure 4 – a. load factors and b. redundancy and robustness obtained from deterministic analysis.

As their concept suggests, the indicators R_u and R_d, also called the system reserve ratios, are useful to measure the influence of the damage of the component's system (local damage) on the overall structural system. Thus, the results presented in Figure 4b. can be interpreted as a stronger influence of the local damage on the overall structure in the early years of the structure's life.

The reliability-based indicators are divided into Part I to Part III (see Figure 5) for a better visualization since the values obtained have large differences in scales. The indicator $\Delta\beta_u$ gives a measure of the safety difference between the intact system and the tendons. The increasing values with time (see Figure 5a) are attributed to the fact that the tendons' reliability drops faster than the safety of the overall bridge system. Therefore, its contribution to the overall structure reliability is smaller once the corrosion in these components has been initiated. On the other hand, the indicator β_r exhibited a decrease over time (see also Figure 5a), given that the difference between intact and damaged systems' reliability increases with prolonged exposure of the structure to chloride.

Reliability-based indicators

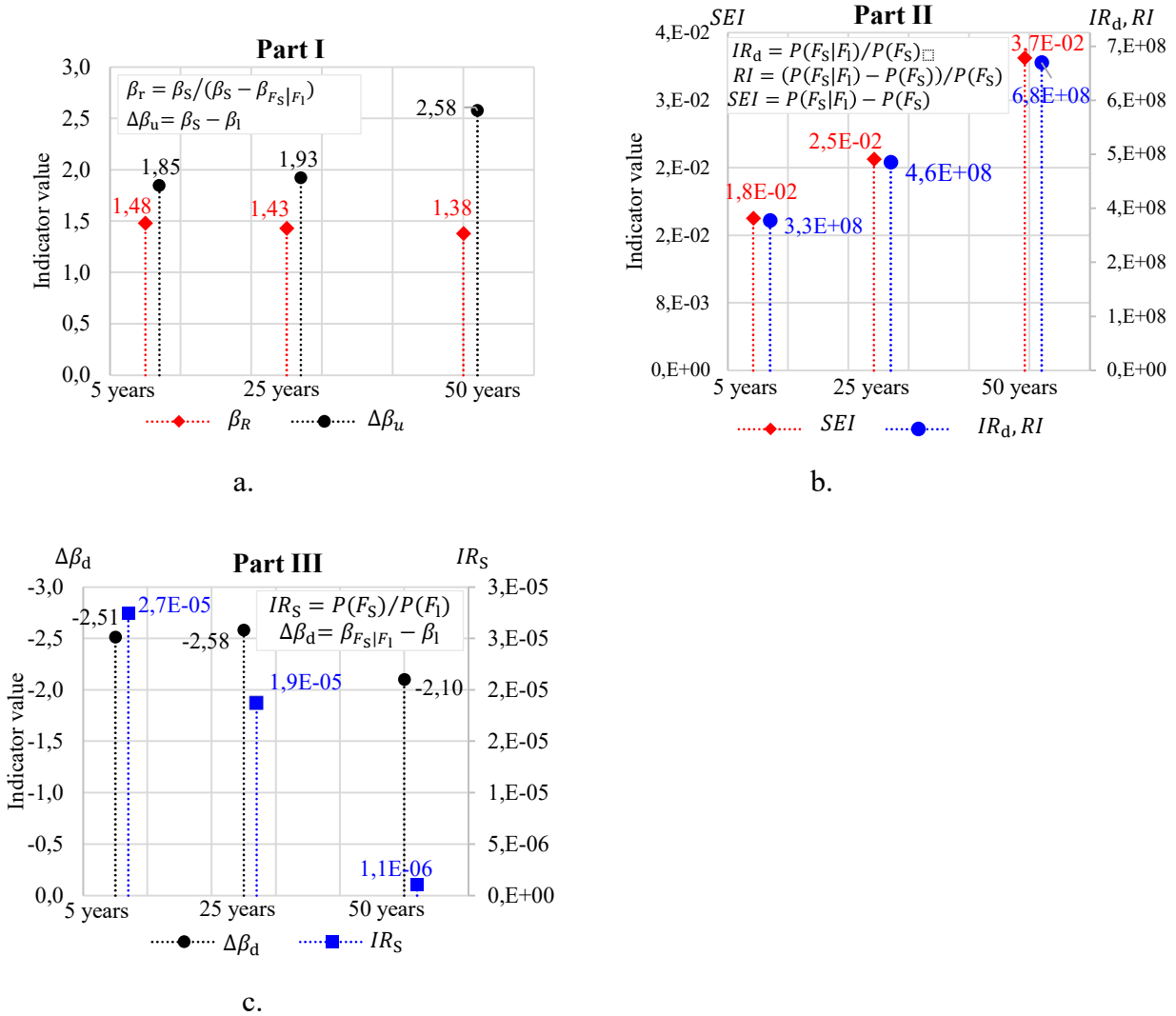

Figure 5 – Indicators obtained from the reliability analysis divided into a. Part I b. Part II and c. Part III.

Given the small value of $P(F_S)$, the indicator RI converged to the same numerical values as IR_d. Additionally, the indicator SEI, which provides a non-normalized version of RI, exhibited the same behavior in time as RI and IR_d, but in a smaller scale (see Figure 5b). These three indicators are measures of the tendons' importance in the overall bridge system's reliability. Thus, the increasing values over time result from the higher influence of the tendons' failure in the bridge's safety, i.e., higher $P(F_S|F_T)$ values.

The indicator IR_S provides the ratio between intact system' and tendons' failure probability. When the tendons lose reliability, the IR_S decreases, indicating a loss of element's importance in the overall bridge system's reliability. On the other hand, decreasing values of $\Delta\beta_d$, i.e., more negative values, indicate a higher gap between the system reliability given element failure and the tendons reliability.

Reliability-based measures are less straightforward than deterministic measures, and their values depend on the random variables considered and their probabilistic properties. As can be seen, these indicators can be obtained by comparing the reliability of the local damage and the intact or damaged systems in different ways. Each comparison provides a different measure, with different

magnitudes and different interpretations. For instance, the indicator $\Delta\beta_u$ shows that with time, as the tendons lose capacity and reliability, their importance in the system decreases representing better system performance. Similarly, the indicator IR_S shows their contribution to the system's reliability decreases for higher tendons failure probability.

On the other hand, indicators in Figure 5b show that the elements' importance increases over time, which is interpreted as a higher impact of the tendons' failure on the overall system's reliability. Therefore, the system performance decays towards the end of the structure's service life. Moreover, the indicator $\Delta\beta_d$ provides the difference in reliability between the damaged system and the tendons. Their values show, among the different analyzed points in time, that the element loses impact on the system's reliability towards the end of the service life.

Risk-based indicators

The risk-based approach was implemented to obtain the robustness index I_{rob}, and the results are shown in Figure 6. The value of I_{rob} decreases over time, attributed to a higher influence of the indirect risks towards the end of the service life, which is caused by the increased failure probability of the damaged bridge system. The decreasing robustness indicates that continuous deterioration over time, increases the probability of high indirect consequences. Following the definitions of redundancy, robustness and importance given in Section 1, it can be affirmed that some of the calculated indicators revealed redundancy levels or elements importance instead of robustness since damage levels are not considered in their mathematical definition.

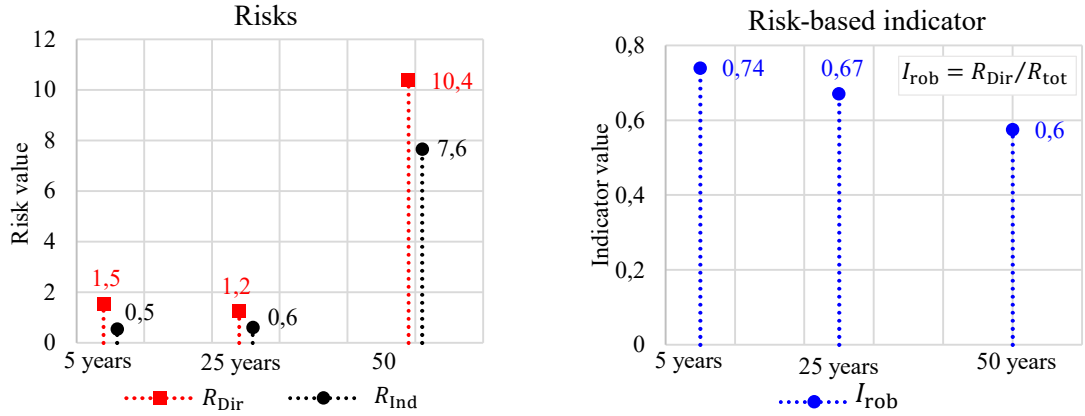

Figure 6 – a. risks and b. robustness values obtained from risk analysis.

4.7 Discussion

The indicators obtained through the three approaches (deterministic, reliability-based, and risk-based) offer different insights into structural integrity and performance, even though they all aim to measure similar properties.

The deterministic measures quantify capacity ratios between structural systems (intact or damaged) and elements, giving a straightforward idea of how much more capacity the structure has if it is considered not only the weakest element but all elements in the system. On the other hand, probabilistic-based measures provide insights into safety level changes in the structural system given different scenarios. Although these measures provide a better overview of the

structure integrity, interpreting them is more complicated due to the magnitude of the measures when working with small probabilities of failure. In this case, it is easy to magnify the redundancy and robustness levels if the reliability index is used instead. Furthermore, the implemented risk-based indicator is easy to interpret since its values vary from 0 to 1, and it is possible to see how the indirect and direct risks impact the robustness levels of the structure.

The primary distinction among these methods lies in the complexity of their assessments. Deterministic measures are relatively straightforward, making them easy to interpret and apply. They are especially useful in scenarios requiring a quick, clear understanding of structural capacity. In contrast, reliability-based measures introduce a higher level of complexity by incorporating probabilistic analysis, accounting for uncertainties in loads, material properties, and other factors. This approach requires statistical knowledge to interpret correctly. A risk-based approach is more complex. It integrates the failure probability and the respective consequences, offering a holistic view of structural performance and a comprehensive picture of robustness. However, it demands a thorough understanding of both probability and risk assessment. Consequently, the choice of approach should be guided by the specific needs and complexity of the problem at hand.

Deterministic measures suffice for straightforward capacity evaluations; reliability-based measures are more appropriate for detailed safety assessments where the safety levels of existing structures are being questioned. More complex risk-based measures are ideal for a complete understanding of risk and robustness, where the structural failure's impact must be considered.

5. CONCLUSIONS

This paper presents a joint evaluation of deterministic, reliability-, and risk-based indicators for a complex case study. A non-linear FEM model and a metamodel-based methodology were implemented to obtain the indicators. The case study consisted of a prestressed concrete bridge subjected to capacity degradation due to chloride ingress. From the analyses carried out, the following conclusions can be drawn:

The metamodel-based reliability method coupled with the FE model showed an acceptable efficiency according to the number of iterations (n_{calls}); the maximum number of iterations needed was 218, which is a significantly small number in comparison with the computational cost of crude Monte Carlo simulations that can reach up to 1×10^{13} simulations required for values of $P(F_S)=1\times10^{11}$. The prediction uncertainty of the metamodel was considered in the analysis, and its accuracy was verified by the calculations of the fitting and predictability factors, R^2 and Q^2, respectively. The value obtained for all the models was 1.0, which showed that the metamodels had a good fitting to the experimental points and that the model can predict the limit state function $g(\boldsymbol{X})$ for additional points. The good fitting and predictability can be attributed to the kriging exact interpolation nature and the use of the learning function, which aimed to add to the experimental points with high kriging standard deviation (increasing accuracy of the metamodel) and close to the failure zone $g(\boldsymbol{X}) = 0$. Therefore, it can be concluded that the accuracy of the metamodel was verified and that the algorithm can be adapted and applied for similar cases of structures with a high computational cost for FEM.

The reliability value obtained for the intact system was significantly higher than the reliability of the elements and damaged system. This highlights that degradation agents, such as chloride ingress, can increase the structural system's vulnerability to sudden collapses over time.

This study presented several indicators proposed in the literature to quantify redundancy and robustness, and it demonstrated how they can be different in magnitude and interpretation for the same case study. This highlights the importance of having a good understanding of their definition and purpose. Also, it was possible to observe that indicators defined in terms of failure probabilities tend to be either really small or high (e.g., IR_S, IR_d, RI) making their interpretation more difficult. It can be affirmed that nowadays the definition of redundancy is more well-established than robustness and some of the measures seen as robustness indicators, currently are acknowledge as redundancy indicators. Thus, further research in this area is needed to establish measures that can be easily interpreted and applied for the case of existing structural systems or to develop ways of interrelating the existing indicators and facilitating the comparison and interpretation.

6. ACKNOWLEDGEMENTS

This work was supported by the Development Fund of the Swedish Construction Industry (*SBUF*), and by the industry program for research and innovation of construction for the transport sector (*BBT*).

REFERENCES

1. Caprani C C, Melhem M M & Siamphukdee K: "Reliability analysis of a super-t prestressed concrete girder at serviceability limit state to as 5100: 2017". *Australian Journal of Structural Engineering*, Vol. 18 No. 2, 2017, pp. 60–72.
2. Zanini M A, Faleschini F & Pellegrino C: "Cost analysis for maintenance and seismic retrofit of existing bridges". *Structure and Infrastructure Engineering*, Vol. 12, No. 11, 2016, pp. 1411-1427.
3. Wang W, Deng L & Shao X: "Number of stress cycles for fatigue design of simply supported steel I-girder bridges considering the dynamic effect of vehicle loading". *Engineering Structures*, Vol. 110, No. 3, 2016, pp. 70–78.
4. Frangopol D M, Dong Y & Sabatino S: "Bridge life-cycle performance and cost: Analysis, prediction, optimisation and decision making". *Structure and Infrastructure Engineering*, Vol. 13, No. 10, 2017, pp. 1239–1257. https://doi.org/10.1080/15732479.2016.1267772
5. Akiyama M, Frangopol D M & Takenaka K: "Reliability-based durability design and service life assessment of reinforced concrete deck slab of jetty structures". *Journal of Structural* Engineering, Vol. 13, No. 4, 2017, pp. 468–77. https://doi.org/10.1080/15732479.2016.1164725.
6. Deng L, Yan W & Nie L: "A simple corrosion fatigue design method for bridges considering the coupled corrosion-overloading effect". *Engineering Structures*, Vol. 178, No. 1, 2019, pp. 309–317. https://doi.org/10.1016/j.engstruct.2018.10.028.
7. Tu B, Dong Y & Fang Z: "Time-dependent reliability and redundancy of corroded prestressed concrete bridges at material, component, and system levels". *Journal of Bridge Engineering*, Vol. 24, No. 9, 2019, pp. 04019085.

8. Ghosn M, Moses F & Frangopol D M: “Redundancy and robustness of highway bridge superstructures and substructures”. *Structure and Infrastructure Engineering*, Vol. 6, No. 1-2, 2010, pp. 257–278.
9. Zhu B & Frangopol D M: “Reliability, redundancy and risk as performance indicators of structural systems during their life-cycle”. *Engineering Structures*, Vol 41, 2012, pp. 34-49.
10. Biondini F: “A measure of lifetime structural robustness”. *Proceedings*, Structures Congress 2009: Don't Mess with Structural Engineers: Expanding Our Role, Austin, Texas, USA, April-May 2009, pp. 1-9.
11. Straub D & Der Kiureghian A: “Reliability acceptance criteria for deteriorating elements of structural systems”. *Journal of Structural Engineering*, Vol. 137, No. 12, 2011, pp. 1573-1582.
12. Dusenberry D O: “New SEI/ASCE disproportionate collapse mitigation standard”. *Journal of Structural Engineering*, Vol. 148, No. 4, 2022, pp. 04022014.
13. Starossek U & Haberland M: “Approaches to measures of structural robustness”. *Structure and Infrastructure Engineering*, Vol. 7, No. 7-8, 2011, pp. 625–631.
14. Baker J W, Schubert M & Faber M: “On the assessment of robustness”. *Structural Safety*, Vol. 30, 2008, pp. 253-267.
15. Knoll F & Vogel T: “IABSE Structural Engineering Documents, Part 11: Design for Robustness”. Zurich. International Association for Bridge and Structural Engineering, 2009.
16. Ghosn M, Frangopol D M, McAllister T P, Shah M, Diniz S M C, Ellingwood B R, Manuel L, Catbas N, Strauss N A & Zhao X L: “Reliability-based performance indicators for structural members”. *Journal of Structural Engineering*, Vol. 142, No. 9, 2016, pp. F4016002.
17. Brett C & Lu Y: “Assessment of robustness of structures: Current state of research”. *Frontiers of Structural and Civil Engineering*, Vol. 7, 2013, pp. 356-368.
18. Restelli S: “Measure of structural robustness of deteriorating systems”. (PhD Thesis), Politecnico di Milano, Milan, Italy, 2007. (in Italian).
19. Feng Y & Moses F: “Optimum design, redundancy and reliability of structural systems”. *Computers & Structures*, Vol. 24, No. 2, 1986, pp. 239-251.
20. Frangopol D M & Curley J P: “Effects of damage and redundancy on structural reliability”. *Journal of Structural Engineering*, Vol. 113, No. 7, 1987, pp. 1533–1549.
21. Ghosn M & Moses F: “NCHRP report 406: Redundancy in highway bridge superstructures”. Transportation Research Board, National Research Council, Washington D.C., 1998.
22. Liu D, Ghosn M & Moses F: “Redundancy in highway bridge substructures”. NCHRP report 458, Transportation Research Board ,Washington, DC, 2000.
23. Cavaco ES, Casas J R, Neves L A C & Huespe A E: “Robustness of corroded reinforced concrete structures - A structural performance approach”. *Structure and Infrastructure Engineering*, Vol. 9, No. 1, 2010, pp. 42–58.
24. Lind N C: “A measure of vulnerability and damage tolerance”. *Reliability Engineering Systems Safety*, Vol. 48, No. 1, 1995, pp. 1–6.
25. Paliou C, Shinozuka M & Chen YN: “Reliability and redundancy of offshore structures”. *Journal of Engineering Mechanics*, Vol. 116, No. 2, 1990, pp. 359-378.
26. Lorengo M & Ma J: “Development of complementary structural robustness metrics based on failure-induced stress redistribution”. *Engineering Structures*, Vol. 266, 2022, pp. 114555.
27. Anitori G, Casas J & Ghosn M: “Redundancy and robustness in the design and evaluation of bridges: European and north American perspectives”. *Journal of Bridge Engineering*, Vol. 18, No. 12, 2013, pp. 1241-1251.

28. Gaspar B, Teixeira A & Soares C G: "Adaptive surrogate model with active refinement combining kriging and a trust region method". *Reliability Engineering and System Safety*, Vol 165, 2017, pp. 277–291.
29. Saydam D & Frangopol D M: "Applicability of simple expressions for bridge system reliability assessment". *Computers Structures*, Vol. 114, 2013, pp. 59–71.
30. Huang X, Chen J & Zhu H: "Assessing small failure probabilities by AK–SS: An active learning method combining Kriging and Subset Simulation". *Structural Safety*, Vol. 59, 2016, pp. 86-95.
31. Yuan K, Xiao N C, Wang Z & Shang K: "System reliability analysis by combining structure function and active learning kriging model". *Reliability Engineering and System Safety*, Vol. 195, 2020, pp. 106734.
32. Zhu Z & Du X: "Reliability analysis with Monte Carlo simulation and dependent Kriging predictions". *Journal of Mechanical Design*, Vol. 138, No. 12, 2016, pp. 121403.1–121403.11.
33. Xiao N C, Zuo M J & Zhou C: "A new adaptive sequential sampling method to construct surrogate models for efficient reliability analysis". *Reliability Engineering and Systems Safety*, Vol. 169, 2018, pp. 330–338.
34. Jiang C, Qiu H, Yang Z, Chen L, Gao L & Li P: "A general failure-pursuing sampling framework for surrogate-based reliability analysis". *Reliability Engineering and Systems Safety*, Vol. 183, 2019, pp. 47–59.
35. Zhang X, Wang L & Sørensen J D: "REIF: a novel active-learning function toward adaptive Kriging surrogate models for structural reliability analysis". *Reliability Engineering and System Safety*, Vol. 185, 2019, pp. 440-454.
36. Rabi S, Karamchandani A & Cornell C A: "Study of redundancy of near-ideal parallel structural systems". *Proceedings*, 5th International Conference on Structural Safety and Reliability, ASCE, New York, USA, 1989, pp. 975–982.
37. Lotsberg I & Kirkemo F: "A systematic method for planning in-service inspections of steel offshore structures". *Proceedings*, Internation conference on Offshore Mechanics and Artic Engineering, The Hague, Netherlands, March 1989.
38. Gharaibeh E S, Frangopol D M & Onoufriou T: "Reliability-based importance assessment of structural members with applications to complex structures". *Computers and Structures*, Vol. 80, No. 12, 2002, pp. 1113–1131.
39. ATENA Science: "ATENA: Advanced Tool for Engineering Nonlinear Analysis ". *Version 5.9*, Cervenka consulting, 2024. https://www.cervenka.cz/products/atena/.
40. Cervenka V: "Global safety format for nonlinear calculation of reinforced concrete". *Beton und Stahlbetonbau*, Vol. 103, No. 1, 2008, pp. 37-42.
41. Rimkus A, Cervenka V, Gribniak V & Cervenka J: "Uncertainty of the smeared crack model applied to RC beams". *Engineering Fracture Mechanics*, Vol. 233, 2020, pp. 107088.
42. Cervenka V: "Reliability-based non-linear analysis according to fib Model Code 2010". *Structural Concrete*, Vol. 14, No. 1, 2013, pp. 19-28.
43. Šomodíková M, Lehký D, Doležel J & Novák D: "Modeling of degradation processes in concrete: Probabilistic lifetime and load-bearing capacity assessment of existing reinforced concrete bridges". *Engineering Structures*, Vol. 119, 2016, pp. 49-60.
44. Bagge N, Plos M & Popescu C: "A multi-level strategy for successively improved structural analysis of existing concrete bridges: examination using a prestressed concrete bridge tested to failure". *Structure and Infrastructure Engineering*, Vol. 15, No. 1, 2019, pp. 27–53.
45. Strauss A, Bergmeister K, Hoffmann S, Pukl R & Novák D: "Advanced life-cycle analysis of existing concrete bridges". *Journal of Materials in Civil Engineering*, Vol. 20, No. 1, 2008, pp. 9-19.

46. AASHTO: "AASHTO LRFD. Bridge Design Specifications 8th Edition". Washington, DC : American Association of State Highway and Transportation Officials, 2017.
47. Poulsen E: "On a model of chloride ingress into concrete". Nordic Mini seminar Chloride Transport. Department of Building Materials, Chalmers University of Technology, Gothenburg, 1993.
48. Kwon S J, Na U J, Park S S & Jung S H: "Service Life Prediction of Concrete Wharves with Early aged Crack: Probabilistic Approach for Chloride Diffusion". *Structural Safety*, Vol. 31, No. 1, 2009, pp. 75-83.
49. Cervenka V, Jendele L & Červenka J: "ATENA Program Documentation–Part 1". Cervenka Consulting sro, 2000.
50. Zhang X, Wang L & Sørensen J D: "AKOIS: an adaptive Kriging oriented importance sampling method for structural system reliability analysis". *Structural Safety*, Vol. 82, 2020, pp. 101876.
51. Imam B M & Chryssanthopoulos, M K: "Causes and consequences of metallic bridge failures". Structural Engineering International, Vol. 22, No. 1, 2012, pp. 93-98. https://doi.org/10.2749/101686612X13216060213437
52. Björnsson I: "Holistic approach for treatment of accidental hazards during conceptual design of bridges-A case study in Sweden". *Safety Science*, Vol. 91, 2017, pp. 168-180.
53. Trafikverket: "Analysis method and socio-economic calculation values for the transport sector: Asek 7.0". ("Analysmetod och samhällsekonomiska kalkylvärden för transportsektorn: Asek 7.0"). Sweden, 2020. (In Swedish).
54. Wong S M, Onof C J & Hobbs R E: "Models for evaluating the costs of bridge failure". *Bridge Engineering*, Vol. 158, No. BE3, 2005, pp. 117-128.
55. Decó A & Frangopol D M: "Risk assessment of highway bridges under multiple hazards". *Journal of Risk Research*, Vol. 14, No. 9, 2012, pp. 1057-1089.
56. Yanaka M, Hooman Ghasemi S & Nowak A S: "Reliability-based and life-cycle cost-oriented design recommendations for prestressed concrete bridge girders". *Structural concrete*, Vol. 17, No. 5, 2016, pp. 836-847.
57. AAHSTO: "A policy on geometric design of rural highways". American Association of State Highway Officials, Washington, D.C, USA, 1965.
58. Kytölä U & Laaksonen A: "Prediction of Restraint Moments in Precast, Prestressed Structures Made Continuous". *Nordic Concrete Research*, Vol. 59, No. 1, 2018, pp.73-93.
59. Akgül F & Frangopol D M: "Lifetime performance analysis of existing prestressed concrete bridge superstructures". *Journal of Structural Engineering*, Vol. 130, No. 12, 2004, pp. 1889–1903.
60. Al-Harthy A S & Frangopol D M: "Reliability assessment of prestressed concrete beams". *Journal of Structural Engineering*, Vol. 120, No. 1, 1994, pp. 180–199.
61. CEB-FIP: "Model code for concrete structures. Comité Euro-International du Béton". Secretariat Permanent, Case Postale, 88, 1993.
62. Hadidi A, Azar B F & Rafiee A: "Structural reliability of prestressed UHPC flexure models for bridge girders". *Journal of Bridge Engineering*, Vol. 15, No. 1, 2010, pp. 65–72.
63. Nowak A S & Collins K R: "Reliability of structures". CRC Press, Taylor and Francis, 2012.
64. Strauss A, Hoffmann S, Wedner R & Bergmeister K: "Structural assessment and reliability analysis for existing engineering structures, applications for real structures". *Structure and Infrastructure Engineering*, Vol. 5, No. 4, 2009, pp. 277–286.
65. JCSS: "JCSS Probabilistic Model Code: Joint Committee on Structural Safety", Denmark, 2001.
66. Bastidas-Arteaga E, Bressolette P, Chateauneuf A & Sánchez-Silva M: "Probabilistic lifetime assessment of RC structures under coupled corrosion–fatigue deterioration processes". *Structural safety*, Vol. 31, No. 1, 2009, pp. 84–96.

67. Dias-da Costa D, Neves L, Gomes S, Hadigheh S & Fernandes P: "Time-dependent reliability analyses of prestressed concrete girders strengthened with CFRP laminates". *Engineering Structures*, Vol. 196, 2019, pp. 109297.
68. Jones M: "Repair of Impact Damaged Prestressed Bridge Girders with Strand Splices and Fabric Reinforced Cementitious Matrix Systems". (Master's Thesis), Virginia Tech, Blacksburg, VA, USA, 2015.
69. WHO: "Global Status Report on Road Safety". World Health Organization. 2018.